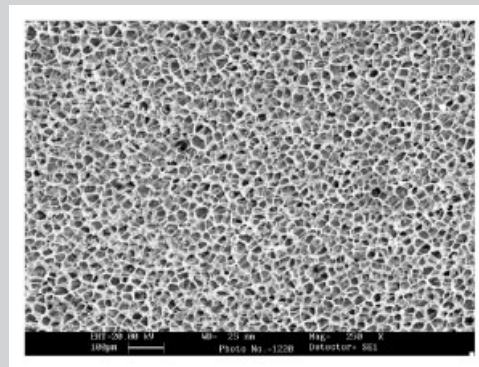


**Summary:** In order to produce modified poly(lactic acid) (PLA) resins for applications requiring high melt viscosity and elasticity (e.g., low-density foaming, thermoforming), a commercial PLA product has been reactively modified in melt by sequentially adding 1,4-butanediol and 1,4-butane diisocyanate as low-molecular-weight chain extenders. By varying amounts of the two chain extenders associated to the end group contents of PLA, three resulted samples were obtained. They were then structurally characterized by FTIR spectroscopy and molecular structure analysis. Their thermal, dynamic mechanical thermal properties and melt viscoelastic properties were investigated and compared along with unmodified PLA. The results indicated that chemical modification may be characterized as chain scission, extension, crosslinking, or any combination of the three depending on the chain extender amounts. The increase of PLA molecular weight could be obtained by properly controlling amounts of two chain extenders. The samples with increased molecular weights showed enhanced melt viscosity and elasticity. Such property improvements promised a successful application for

modified PLA in a batch foam processing by producing foams with reduced cell size, increased cell density and lowered bulk foam density in comparison with plain PLA foam.



Cellular morphology of a modified PLA foam.

## Reactively Modified Poly(lactic acid): Properties and Foam Processing

Yingwei Di,\*<sup>1</sup> Salvatore Iannace,<sup>1</sup> Ernesto Di Maio,<sup>2</sup> Luigi Nicolais<sup>1,2</sup>

<sup>1</sup>Institute for Composite and Biomedical Materials (IMCB-CNR), Piazzale Tecchio 80, 80125 Napoli, Italy  
Fax: (+39) 081 7682404; E-mail: di@unina.it

<sup>2</sup>Department of Materials and Production Engineering, University of Napoli "Federico II," Piazzale Tecchio 80, 80125 Napoli, Italy

Received: March 2, 2005; Revised: July 6, 2005; Accepted: August 3, 2005; DOI: 10.1002/mame.200500115

**Keywords:** chain extenders; foams; poly(lactic acid) (PLA); reactive modification

### Introduction

Poly(lactic acid) (PLA) is a biocompatible, environmentally friendly biodegradable thermoplastic polymer which is now finding commercial use in single-use disposable items, in addition to the established applications in medical implant, sutures, and drug delivery systems.<sup>[1]</sup> The need for biodegradable polymers in the context of designing materials for the environment is also opening up new markets of opportunities for PLA.<sup>[2]</sup> However, one of the limitations for using PLA is its processing instability, i.e., thermal, oxidative, and hydrolytic degradations may occur during processing – leading to the cleavage of polymer chains, and hence to a decrease in molecular weight.<sup>[3]</sup> All these degradation processes result in a deterioration of the

rheological properties, which should be avoided for processing purpose, especially when high levels of extensional viscosity and elasticity are required, such as for blow molding and extrusion foaming. Another shortcoming of PLA is its very low melt viscosity, which may also limit its blow molding and foaming processabilities.

To overcome such shortcomings, attempts to control the melt rheology of PLA by means of increasing molecular weight to compensate for the molecular weight decrease caused by processing degradation and to increase the melt viscosity have motivated considerable research efforts. The free radical branching/linking of PLA has been tried in the melt mixing in an extruder or in a kneader in the presence of trace amounts of various peroxides as radical initiators.<sup>[4–7]</sup> The solid-state postpolymerization technique has also been

used to obtain high-molecular-weight PLA.<sup>[8]</sup> Recently, efforts on chain extending of low-molecular-weight PLA or lactic acid oligomers by using functional additives, so-called “chain extenders,” to link the end groups of these low-molecular-weight PLA have been reported.<sup>[9–12]</sup> The prime objective in these studies was to obtain high-molecular-weight PLA, tailored for specific processes. For this purpose, the authors have synthesized low-molecular-weight PLA or its oligomers and then carried out chemical modification with chain extenders through coupling of these molecules to obtain chain-extended/branched PLA. These chain extension reactions not only offered the opportunity for enhancement of physical and chemical properties by increasing the molecular weight but also introduced new functional groups onto the PLA backbone paving the way for preparation of composites, laminates, coated items, and blends/alloys with improved properties and cost effectiveness.<sup>[13]</sup> In the meantime they are economically advantageous because they can be carried out in the melt, with only low amounts of chain extending agents, and separate purification steps are not required.

In this paper, we reported our effort to achieve increase in molecular weight for a commercial PLA product by using chain extenders, with expectation of improving its viscoelastic properties for foam processing. To our best knowledge, it is the first paper on treating a commercial PLA with chain extenders. The very high reactivity of the isocyanates has encouraged us to select 1,4-butane diisocyanate (BDI) as chain extender for coupling and chain extension of PLA molecules. However, in our previous experience, the molecular weight increase in only BDI-treated PLA was not found. The similar founding was also reported in LA oligomer chain extension that could be attributed to the presence of carboxyl groups.<sup>[12]</sup> In order to effectively use BDI in PLA chain extension, in this study, we used two chain extenders: 1,4-butanediol (BD) and BDI to modify the commercial PLA in two steps. In the first step, BD was selected as first coupling agent and acid value (AV) reducer to link carboxyl groups of PLA and then, in the second step, BDI was added to let it react with hydroxyl end groups of PLA to achieve chain-extended PLA. The different amount ratios of two chain extenders were used to investigate their effect on the structure of modified PLA samples which were then characterized and foamed in a batch foaming process.

## Experimental Part

### Materials and Reactive Modification

Poly(lactic acid) (L-lactide > 92 wt.-%) under the commercial name of NatureWorks<sup>®</sup> from Cargill-Dow, UK was used in this study. BD, BDI, and tin(II) 2-ethylhexanoate from Aldrich-Sigma were used as received.

The reactive modification of PLA was carried out in a Haake melt mixer at 170 °C under nitrogen atmosphere and 60 rpm by

sequentially mixing with BD (with trace amount of tin(II) 2-ethylhexanoate as catalyst, 0.05 wt.-% of PLA) and BDI. Three modified PLA samples were obtained by using different amount ratios of COOH/BD and OH/BDI, where OH content of PLA was determined by standard titrimetric method (DIN 53240) and COOH content was calculated from the AVs determined by titration (detailed below). Sample 1 (M1): COOH/BD = 2:1, OH/BDI = 2:1, i.e., equimolar amount of BD and COOH, BDI and OH, respectively; sample 2 (M2): COOH/BD = 2:1, OH/BDI = 1:1, i.e., BDI amount was excessive compared to M1; sample 3 (M3): COOH/BD = 1:1, OH/BDI = 2:1, i.e., BD was excessive compared to M1. Before the typical experiment, the reaction time in two steps for each sample has been determined as follows. In the first step, the variation of acid number in blending PLA and BD was monitored by taking out samples at 1-min interval and analyzing acid number, and the time at minimum acid number was determined as the adding point of BDI for starting the second step reactive modification. Then the change in mixing torque was taken as an indicator of modification process and the time at maximum torque was taken as the reaction stop point. Typically, for a linking reaction, 50 g of the dried PLA powder was loaded into the preheated Haake melt mixer. After the PLA was completely molten, BD (with tin (II) 2-ethylhexanoate) of predetermined amount was first mixed with PLA. After the determined reaction time for the first step, the required amount of BDI was added. Then, after the predetermined reaction time passed, the mixer was stopped and the modified PLA was hot pressed for further characterization. The original PLA was also processed under the same conditions without modification for the reason of comparison and named plain PLA hereafter.

### Characterization

FTIR spectra were obtained using a Nicolet FTIR spectroscopy (Nexus 670). Each spectrum was recorded with a total of 32 scans with the resolution of 4 cm<sup>-1</sup>. For the FTIR samples, the plain PLA and modified PLA were pressed into about 20 μm thick films under 100 MPa pressure at 170 °C.

The molecular weights of samples were characterized by GPC (Waters Alliance HPLC Systems, model 2695) equipped with microstyrage<sup>™</sup> columns at 25 °C. It was calibrated with polystyrene standards that covered the range of molecular weight, 1 000 to 1 million. THF was used as the eluent at the flow rate of 1 mL · min<sup>-1</sup>.

Acid values, defined as the weight in milligrams of KOH required to neutralize 1 g of the polymer, were determined by titrimetric methods. The solution of each sample in chloroform was titrated against 0.01 M KOH in ethyl alcohol solution in the presence of phenolphthalein as indicator. The number of COOH end groups present in each sample was calculated.

The thermal properties of samples were analyzed by DSC on DSC2910 (TA Instruments, USA). Samples of about 10 mg were weighed and sealed in the aluminum DSC pans and placed in the DSC cell. They were first heated from 20 to 200 °C at a rate of 10 °C · min<sup>-1</sup> under nitrogen atmosphere. The samples were kept at 200 °C for 3 min to eliminate the previous heat history and subsequently cooled to 20 °C at 10 °C · min<sup>-1</sup>. They were then heated again to 200 °C at 10 °C · min<sup>-1</sup>.

This second heating process was regarded as melting scan for the analysis. The glass transition temperature ( $T_g$ ), crystallization temperature ( $T_c$ ), and melting temperature ( $T_m$ ) were determined from the second heating scans. The  $T_c$  and  $T_m$  were taken at the peak value of the respective exothermic and endothermic graphs, and the  $T_g$  at the midpoint of heat capacity changes. When multiple endothermic peaks were found, the peak temperature of the main endotherm was taken as  $T_m$ .

Dynamic mechanical thermal analysis on each sample was performed on a dynamic mechanical analyzer: model DMA983 of TA Instruments, USA. The testing was carried out in three-point bending mode at a vibration frequency of 1 Hz in temperature range from 0 to 160 °C at a heating rate of 10 °C · min<sup>-1</sup> in N<sub>2</sub> atmosphere. Sample dimensions were 20 mm in length, 5 mm in width, and 1 mm in thickness.

Dynamic rheological measurements were carried out using an advanced rheometric expansion system (ARES) rheometer from Rheometric Inc, USA. The measurements were performed in an oscillatory shear mode using parallel plate geometry of 25 mm in diameter at 170 °C under nitrogen atmosphere. Frequency sweeps between 0.01 and 100 rad · s<sup>-1</sup> were carried out at low strains (0.1–10%) which have been shown to be within the linear viscoelastic range of the measured samples. Specimens were placed between the preheated plates at experimental temperature and were allowed to equilibrate prior to each frequency sweep run.

#### Foaming Processing and Cellular Structure Analysis

The physical foaming (batch process) was conducted in a high-pressure stainless steel autoclave made by HiP, PA, USA. The plain and modified PLA, punched from a compression-molded plaque with a diameter of 10 mm and thickness of 1 mm, were dried, weighed, and placed on the sample holder inside the autoclave. The blowing agent used in this study was mixture of compressed CO<sub>2</sub> and N<sub>2</sub> (20/80), Aligal<sup>®</sup> by Air Liquide, Italy. Before a typical experiment, the autoclave was flushed with blowing agent for a few seconds and then pressurized with blowing agent and heated to the solubilization temperature (170 °C). The pressure of blowing agent at this temperature was adjusted to the desired saturation pressure (16 MPa). The solubilization time, about 4 h, was maintained to ensure equi-

librium absorption of blowing agent by the samples and then the temperature was cooled down at circa 5 °C · min<sup>-1</sup> to the foaming temperature (110 °C) and the pressure was rapidly reduced to atmosphere pressure by opening the valve of autoclave. After that the autoclave was opened and the foamed samples were cooled naturally to room temperature and kept in desiccator at room temperature.

The cell structure of the resulted foams was analyzed by using a LEICA scanning electron microscopy (SEM) model S440. The SEM samples were prepared by cryogenically cutting the obtained foam samples and gold sputtering the fractured cross sections. The average cell size,  $d$  (in mm), was obtained by measuring the maximum diameter of each cell perpendicular to the skin from SEM micrographs. At least 50 cells in SEM micrograph were measured. The bulk densities of both prefoamed,  $\rho_p$ , and postfoamed,  $\rho_f$ , samples in g · cm<sup>-3</sup> were estimated by using the method of buoyancy. The cell densities,  $N_c$ , in cells · cm<sup>-3</sup>, are defined using Equation (1) by assuming the cells are spherical:<sup>14</sup>

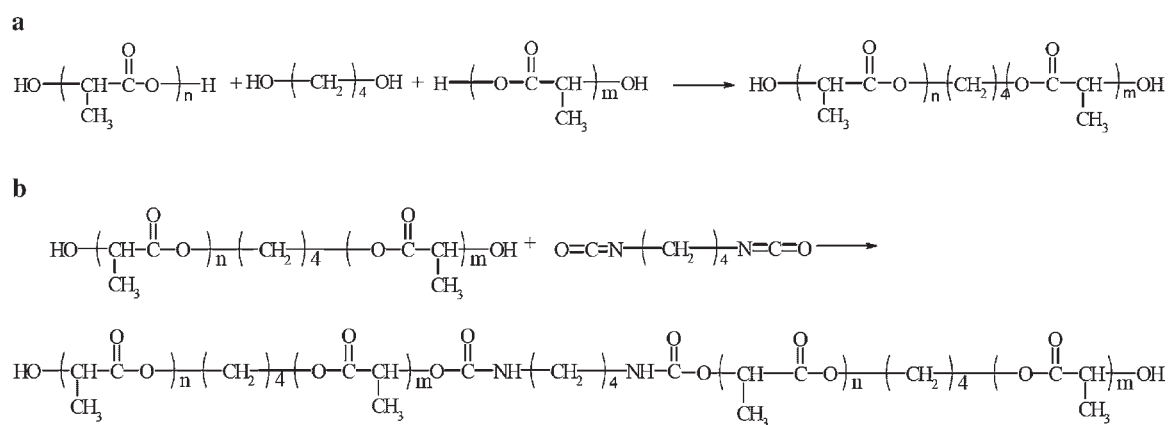
$$N_c \approx 10^4 [1 - (\rho_f/\rho_p)]/d^3 \quad (1)$$

## Results and Discussion

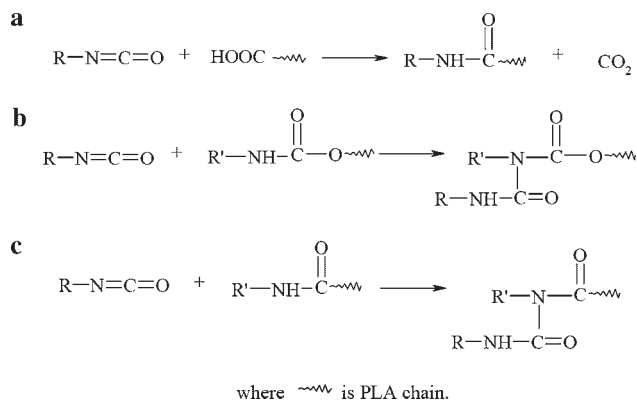
### Chain Extending Reactions and FTIR, GPC Analysis

In this study, a typical two-step reactive modification method was applied to obtain chain-linked high-molecular-weight PLA. In first step, the plain PLA melt was allowed to first react with BD in the presence of trace amount of tin(II) 2-ethylhexanoate to obtain hydroxyl terminated PLA (OH-PLA) [Scheme 1(a)]. The variation of PLA AVs was monitored and found to gradually reduce with reaction time and then seemed to level-off or increase. At the point when AV stopped decreasing, BDI was fed to let the chain linking between OH-PLA and BDI take place, leading to the formation of urethane [Scheme 1(b)].

However, it is well known that the –NCO groups of isocyanate readily react with every active hydrogen in the reacting system. Because of equilibrium reaction there are always some residual carboxyl groups in the reaction



Scheme 1.



Scheme 2.

system. Consequently, besides engaging in urethane formation, BDI can also react with carboxyl group residuals leading to amide bond [Scheme 2(a)]. The urethane and amide groups can further react with additional isocyanate. Such reactions can cause crosslinks in PLA [Scheme 2(b) and (c)].

An inspection of chain coupling reactions for modified PLA was carried out on FTIR in the spectral regions of  $3700\text{--}3150\text{ cm}^{-1}$  and  $1750\text{--}1450\text{ cm}^{-1}$  as shown in Figure 1. The spectrum of unmodified PLA is also presented [Figure 1(a)], in which the absorption band around  $3660\text{ cm}^{-1}$  is attributed to the free hydroxyl stretching vibration of PLA end groups and that around  $3500\text{ cm}^{-1}$  is assigned to hydrogen bonding associated with hydroxyl group; the broad band between  $3300$  and  $3150\text{ cm}^{-1}$  is for carboxylic groups of PLA. For the modified samples [Figure 1(b–d)], the diminishment of  $\text{--OH}$  absorption peaks and disappearance of  $\text{--COOH}$  band, compared to the plain PLA [Figure 1(a)], were evident, showing the consumption

of end groups of OH and COOH after modification. Furthermore, the appearance of the characteristic peak of NH groups ( $3350\text{ cm}^{-1}$ ), of a medium to weak intensity [Figure 1(b–d)], indicates the formation of urethane and amide groups. In the region of  $1800\text{--}1400\text{ cm}^{-1}$  the urethane bond formed by the reaction between  $\text{--OH}$  and  $\text{--NCO}$  groups is coincident with the carbonyl absorption ( $1760\text{ cm}^{-1}$ ) of the PLA, but an amide II band of urethane bond also appears at  $1525\text{ cm}^{-1}$  [Figure 1(b–d)]. When the isocyanate group reacts with the carboxyl group, amide I absorption bands of the amide bond appear in the region of  $1700\text{--}1650\text{ cm}^{-1}$ , which are seen in Figure 1(b–d) as shoulders around  $1690\text{ cm}^{-1}$ . These observations suggested that the coupling reactions between PLA end groups and chain extenders have taken place.

The GPC results of plain and modified PLA are summarized in Table 1. It is clearly shown that the molecular weights (both,  $\bar{M}_w$  and  $\bar{M}_n$ ) for samples M1 and M2 were increased compared to plain PLA because of chain extension. The effect of excess BDI can also be seen by the higher  $\bar{M}_w$  and  $\bar{M}_n$  for M2 compared to M1, caused by more linking reactions as shown in Scheme 2.  $\bar{M}_n$  for sample M3 was lowered which could be attributed to the excessive BD added, inducing more PLA degradation through hydrolysis. However, the molecular weight increase in M1 and M2 was not expected as theoretical prediction (Scheme 1), indicating that chain scission (caused by degradation) has also taken place besides the chain extension.

### Thermal Properties

Thermal properties of plain and modified PLA were first studied by DSC. The corresponding heating thermograms are shown in Figure 2 and the results are summarized in

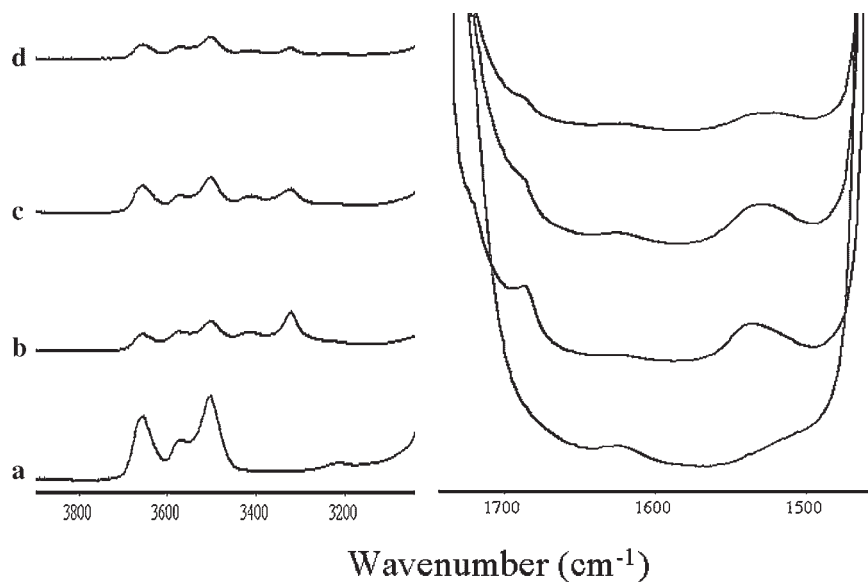


Figure 1. FTIR spectra of (a) plain PLA, (b) M1, (c) M2, and (d) M3.

Table 1. Molecular weight of plain and modified PLA from GPC.

Sample	$\bar{M}_n/10^3$	$\bar{M}_w/10^3$	$\bar{M}_w/\bar{M}_n$
	$\text{g} \cdot \text{mol}^{-1}$	$\text{g} \cdot \text{mol}^{-1}$	
Plain PLA	57	124	2.2
M1	84	225	2.7
M2	107	308	2.9
M3	48	156	3.3

Table 2. Compared to plain PLA, the M1 and M2 samples showed slightly higher glass transition temperatures ( $T_g$ ) due to the higher molecular weight and chain crosslinking. Crosslinking increases the  $T_g$  of the polymer by introducing restrictions in chain mobility.<sup>[12]</sup> For M1 and M2 samples, a broad band of crystallization appeared on each melting curve, which is indicative of much reduced ability for the molecules to crystallize as a result of modification.  $T_g$  of M3 is lower than PLA that was assumed to be caused by the plasticization effect of the degraded PLA chains acting as plasticizers. As seen in Figure 2 the melting endotherm of M3 showed two distinct peaks as a result of crystal lamellar rearrangement during crystallization. This is a typical behavior for plasticized thermoplastics: a “shoulder” or low-temperature peak is formed on the melting endotherm of the main crystallites.<sup>[15]</sup> A significant decrease in the  $T_m$  was also observed for the modified PLA compared to plain PLA as a result of the introduction of defects in the crystal lamellae by crosslinking after modification. These results are in agreement with those reported on PET and PBT resins chain extended by low  $\bar{M}_w$  difunctional epoxides.<sup>[16,17]</sup>

### Dynamic Mechanical Thermal Properties

The efficiency of the chain-linking reaction was also appraised through DMA tests. The dynamic storage modulus

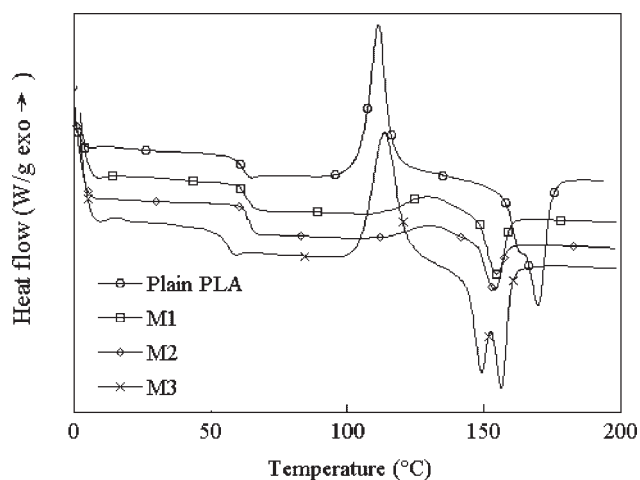


Figure 2. DSC melting thermograms of plain and modified PLA samples.

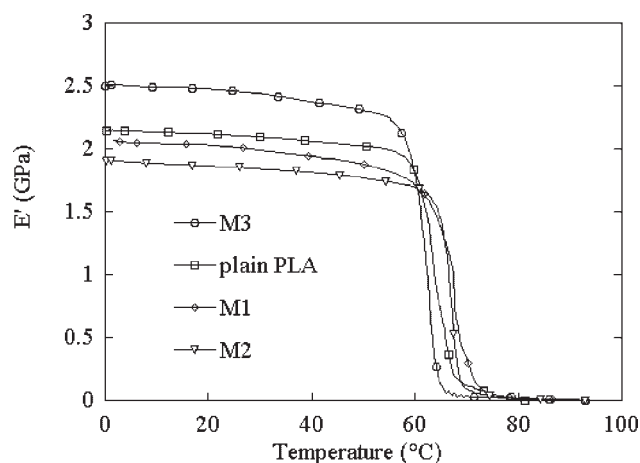
Table 2. Thermal properties of plain and modified PLA samples.

Sample	$T_g$	$T_c$	$T_m$
	$^{\circ}\text{C}$	$^{\circ}\text{C}$	$^{\circ}\text{C}$
PLA	61.8	111.5	169.6
M1	63.2	129.1	154.5
M2	63.7	130.2	153.8
M3	55.7	113.8	156.3

( $E'$ ) as a function of temperature for plain and modified PLA samples is shown in Figure 3. Before reaching to glass transition region, M1 and M2 showed lower  $E'$  than plain PLA. It is well known, generally, that the introduction of crosslinks reduces the molecular packing and crystallization, leading to a more or less amorphous materials with a lower modulus and hardness. The M1 and M2 have more content of crosslinks than plain PLA; therefore, they exhibited lower  $E'$  values. M3 has a higher  $E'$  than plain PLA because of higher crystallinity as seen from first DSC heating scans (not shown) as a result of plasticization. As temperature increases, all DMA curves show a marked drop in  $E'$ , corresponding to the glass transition ( $T_g$ ). For M3 and plain PLA, the drop starts earlier than M1 and M2, implying lower  $T_g$  than M1 and M2 as same as we have seen from DSC analysis.

### Rheological Properties

Dynamic rheological frequency sweeps were used to determine differences in the structures of the plain and modified PLA samples. Figure 4 shows their complex viscosity as a function of frequency. It can be seen that plain PLA exhibits typical Newtonian behavior in the low-frequency region and small shear thinning starts up to  $10 \text{ rad} \cdot \text{s}^{-1}$  that is a characteristic for linear polymers. M3


 Figure 3. Temperature dependence of  $E'$  for plain and modified PLA samples.

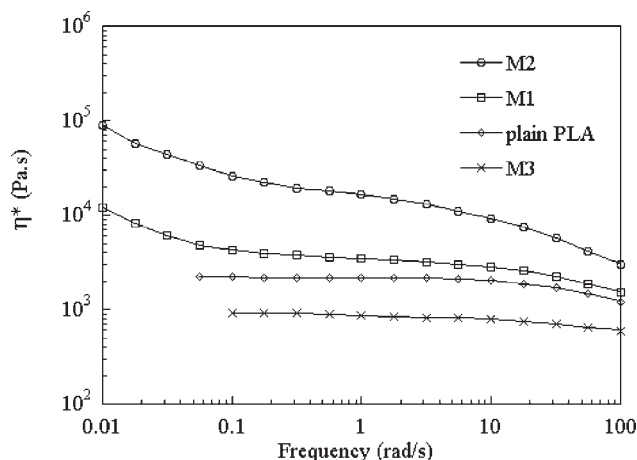


Figure 4. Complex viscosity curves for plain and modified PLA samples.

shows the similar behavior but lower complex viscosity than the plain PLA that could be attributed to the lubrication effect of degraded low-molecular-weight parts in it. However, M1 and M2 samples have much higher complex viscosities than plain PLA and show non-Newtonian behavior in the tested frequency range with shear thinning already at low frequencies. The high viscosities for M1 and M2 are caused by molecular entanglements with the increase of molecular weights and the strong shear thinning behavior is typical for crosslinked or broad molecular weight distribution PLA.<sup>[18,19]</sup> In addition to molecular entanglements, strong physical interaction between ester groups also play a role in rheological behavior of crosslinked polyesters.<sup>[20]</sup> That is, the physical bonding through ester groups may lead to formation of pseudostructures, which would increase with increasing molecular weights of PLA. Consequently, low-frequency shear thinning is more prominent in M1 and M2. The viscosity of M2 is higher than that of M1 because of its higher crosslinking content induced by excessive addition of BDI during chain extension process.

Such modification has also caused a dramatic increase in storage modulus,  $G'$ , and loss modulus,  $G''$ , for M1 and M2. As seen in Figure 5,  $G'$  of M1 and M2 are overall higher than that of plain PLA and show less frequency dependence at low-frequency range. This is attributable to more entanglements and the previously suggested pseudostructures through formation of physical networks at high molecular weights. That is, over a range of frequencies the balance between viscous and elastic properties is retained because of the existence of gel-like pseudostructures, which can withstand the shear force. Hence, chain interactions play a more important role and give rise to higher storage modulus for M1 and M2, resulting in yield stress that is indicated by a plateau in  $G'$  curve at low-frequency range.<sup>[21]</sup> The increase in the storage modulus means improved elasticity for M1

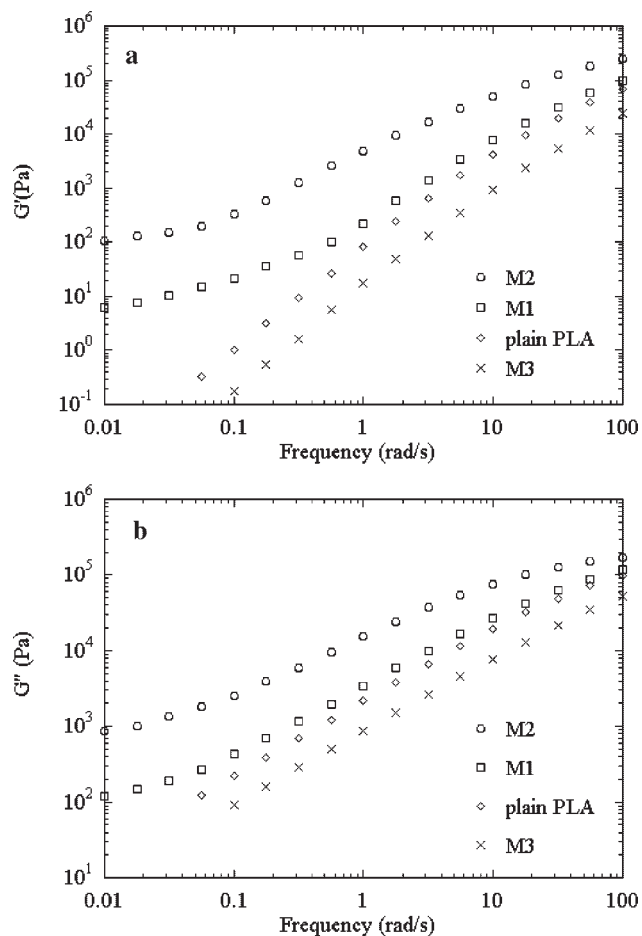


Figure 5.  $G'$  (a) and  $G''$  (b) vs. frequency for plain and modified PLA samples.

and M2 samples. The  $G''$  of M1 and M2 show a similar trend as  $G'$  that are higher than those of plain PLA and M3. Plain PLA and M3 show typical linear polymer characteristic that  $G'$  and  $G''$  curves show a slope of about 2 and 1, respectively, at low-frequency range. It is known that the melt elasticity has a direct relationship with the melt strength which is an indication of the resistance for a melt to extension.<sup>[22]</sup> In general, the literature suggests that similar modifications in macromolecular structure may give high melt strength and high melt elasticity at the same time.<sup>[23]</sup> Accordingly, such chemical modification has improved both melt viscosity and elasticity/strength for PLA as seen in samples M1 and M2.

### Foam Processing and Cellular Structure Analysis

It has been well described that high melt viscosity at low shear rate/frequency, high shear sensitivity, and high melt strength/elasticity are characteristics of resins suitable for blow molding, foaming, and thermoforming.<sup>[24]</sup> Accordingly, the observed improvement in viscous and elastic properties for modified PLA samples has encouraged us to

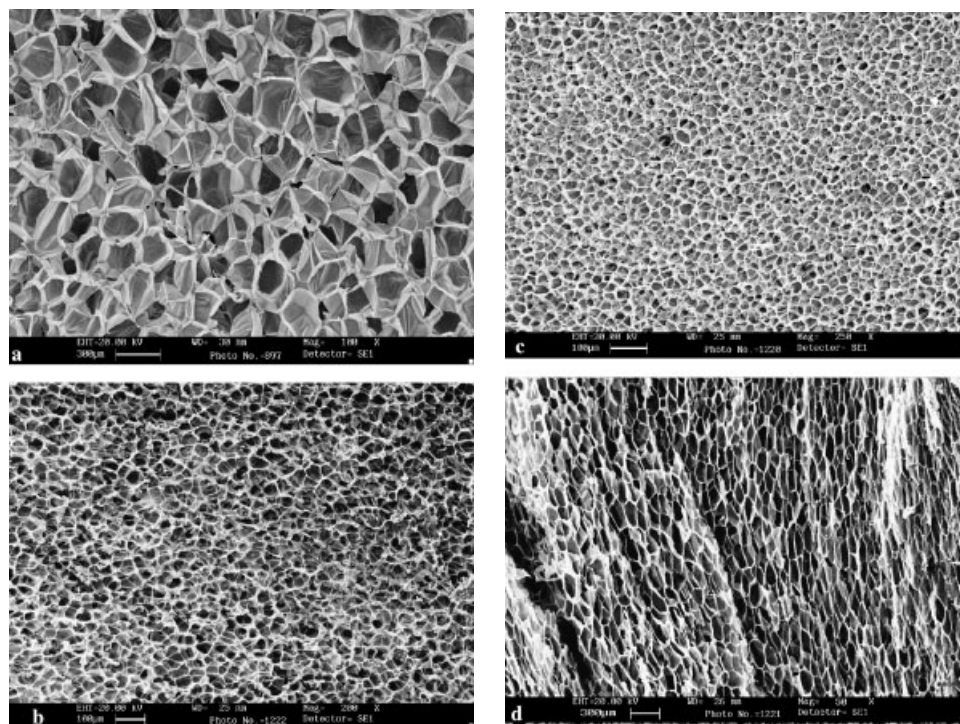


Figure 6. SEM micrographs for foamed plain PLA (a) ( $\times 100$ ) and modified PLA: M1 (b) ( $\times 200$ ), M2 (c) ( $\times 250$ ), and M3 (d) ( $\times 50$ ).

perform foam processing on them. All the resulted foams have a thin and shiny skin layer. It was assumed that this skin layer is formed by phase separation, during the depressurization, of the blowing agent dissolved in polymer matrix. Under the skin layer, the foams have homogeneous morphology, independent of the depth from the surface, implying the sufficient solubilization time. In Figure 6, the SEM micrographs of plain and modified PLA foams processed at the given conditions were shown. cursory examination of these micrographs showed a striking difference that the cell size ( $d$ ) in foams of plain PLA and M3 is similar, but that in M1 and M2 foams is significantly reduced, indicating the modification effect on the foam structure. The results of image analysis on these micrographs are listed in Table 3. We note that the average cell sizes of plain PLA and M3 sample foams are about six and ten times larger than those of M1 and M2 foams, respectively. This behavior is due to the intrinsically high viscosity and elasticity of the M1 and M2 samples which restricted the expansion of cells. For plain PLA and M3 foams cell coalescence and rupture were observed, resulted from their low viscosity and weak elasticity.

As seen in Table 3, the cell densities for M1 and M2 foams are much higher than plain PLA and M3 foams. Such differences could be ascribed to the differences in activation energies for cell nucleation, resulted from differences in polymer surface tension due to chain extension and cross-linking.<sup>[23]</sup> That is, because of high viscosity in M1 and M2,

resistance to bubble growth in them is high and it probably requires less energy to create a new bubble by nucleation than to inflate an existing one by diffusion and mass transfer. For the same reason, the foam of M3 has the least cell density because of its lowest viscosity.

The bulk foam density was also reduced for M1 and M2 foams in comparison to plain PLA foam. But for foamed M3, the foam density is higher than that of plain PLA. Such difference in foam density was assumed to be caused by loss of blowing agent during foaming process, in which there was competition between diffusion and resistance for blowing agent. Under the given foaming conditions in this study, the diffusion of dissolved blowing agent to exterior phases for M3 prevails over plain PLA, M1, and M2 because of its lowest melt strength, resulting in highest foam density in foamed M3. Diffusion of blowing agent to

Table 3. Average cell size, average cell density, and bulk foam density for foamed plain and modified PLA samples.

Sample	Average cell size	Average cell density	Foam density
	$\mu\text{m}$	$10^8 \cdot \text{cm}^{-3}$	$\text{g} \cdot \text{cm}^{-3}$
PLA	227	0.00766	0.125
M1	37	1.866	0.0666
M2	24	6.682	0.0923
M3	223	0.00768	0.179

the exterior is expected for M1 and M2 as well because the polymer matrix surrounding the gas cells is in the rubbery state during foaming. However, the diffusion loss of gas for M1 and M2 is much lower than M3 because of their higher melt resistance. Accordingly, the resulted foams of M1 and M2 have higher foaming grade (lower foam density). The foam density for M2 is a little bit higher than that for M1, which implies that there exists an optimum in foam density control among polymer melt viscosity/elasticity and processing conditions.

## Conclusion

It can be concluded that the commercial PLA could be effectively chain extended/crosslinked by controlling the amounts of two chain extenders for specific application purposes such as highly oriented films and low-density foams. The molecular weights have been increased at BD and BDI contents equal to carboxyl and hydroxyl contents in PLA, respectively. Excessive BD would induce more PLA degradation; however, more BDI content gave rise to more crosslinkings in PLA structure and higher molecular weight. Compared to the plain PLA, such modified PLA samples, i.e., M1 and M2 in this study, showed higher  $T_g$  and low crystallization rate because of the restriction of molecular chain, resulted from the extended/crosslinked chain structure. They have much higher complex melt viscosity and show earlier shear-thinning with a virtual absence of a Newtonian region in the melt viscosity versus shear frequency curve. Their melt elasticity was also increased by showing higher  $G'$  and a plateau over low dynamic frequency range.

The higher viscosity and elasticity for the chain-extended/crosslinked resins allowed the production of PLA foams with smaller cell size, higher cell density, and lower foam density compared to plain PLA. This preliminary study showed that reactive modification with chain extenders as a postprocessing technique provides a new strategy for the design and control of cell structure in PLA

foams and the improvement of PLA melt fabricability for various application purposes.

- [1] D. Garlotta, *J. Polym. Environ.* **2001**, *9*, 63.
- [2] R. Narayan, *ACS Symp. Ser.* **1992**, *476*, 1.
- [3] H. Tsuji, I. Fukui, *Polymer* **2003**, *44*, 2891.
- [4] D. Carlson, P. Dubois, L. Nie, R. Narayan, *Polym. Eng. Sci.* **1998**, *38*, 311.
- [5] D. Carlson, L. Nie, R. Narayan, P. Dubois, *J. Appl. Polym. Sci.* **1999**, *72*, 477.
- [6] A. Sodergard, M. Niemi, J. F. Selin, J. H. Nasman, *Ind. Eng. Chem. Res.* **1995**, *34*, 1203.
- [7] E. Park, H. Cho, M. Kim, J. Yoon, *J. Appl. Polym. Sci.* **2003**, *90*, 1802.
- [8] K. Shinno, M. Miyamoto, Y. Rimura, *Macromolecules* **1997**, *30*, 6438.
- [9] J. Kylma, J. Tuominen, A. Helminen, J. Seppala, *Polymer* **2001**, *42*, 3333.
- [10] W. Zhong, J. Ge, Z. Gu, W. Li, X. Chen, Y. Zang, Y. Yang, *J. Appl. Polym. Sci.* **1999**, *74*, 2546.
- [11] K. Hiltunen, J. V. Seppala, M. Harkonen, *J. Appl. Polym. Sci.* **1997**, *63*, 1091.
- [12] J. Tuominen, J. Kylma, J. Seppala, *Polymer* **2002**, *43*, 3.
- [13] M. H. Hartmann, "High Molecular Weight Polylactic Acid Polymers", in: *Biopolymers from Renewable Resources*, D. L. Kaplan, Ed., Springer, Berlin 1998, p. 367.
- [14] P. H. Nam, P. Maiti, M. Okamoto, T. Kotaka, *Polym. Eng. Sci.* **2002**, *42*, 1907.
- [15] O. Martin, L. Averous, *Polymer* **2001**, *42*, 6209.
- [16] B. Guo, C. M. Chan, *SPE ANTEC* **1998**, *44*, 1653.
- [17] D. N. Bikiaris, G. P. Karayannidis, *J. Appl. Polym. Sci.* **1996**, *60*, 55.
- [18] H. J. Lehermeier, J. R. Dorgan, *Polym. Eng. Sci.* **2001**, *41*, 2172.
- [19] E. S. Kim, B. C. Kim, S. H. Kim, *J. Polym. Sci., Part B: Polym. Phys.* **2004**, *42*, 939.
- [20] H. G. Chae, B. C. Kim, S. S. Im, Y. K. Han, *Polym. Eng. Sci.* **2001**, *41*, 1133.
- [21] Y. Di, S. Iannace, E. Di Maio, L. Nicolais, *J. Polym. Sci., Part B: Polym. Phys.* **2005**, *43*, 689.
- [22] C. B. Park, L. K. Cheung, *Polym. Eng. Sci.* **1997**, *37*, 1.
- [23] M. Xanthos, U. Yilmazer, S. K. Dey, J. Quintans, *Polym. Eng. Sci.* **2000**, *40*, 554.
- [24] M. Xanthos, M. W. Young, G. P. Karayannidis, D. N. Bikiaris, *Polym. Eng. Sci.* **2001**, *41*, 643.